Measurements of magnetic-dipole and electric-quadrupole interaction constants of the 11, 12 and $13^2D_{5/2}$ states in ^{87}Rb by the quantum-beat method

J. Phys. B: At. Mol. Opt. Phys. **22** (1989) 3109-3117. Printed in the UK

Measurements of magnetic-dipole and electric-quadrupole interaction constants of the 11, 12 and $13^2D_{5/2}$ states in ^{87}Rb by the quantum-beat method

M Głódź† and M Kraińska-Miszczak‡

† Institute of Physics, Polish Academy of Sciences, Al Lotników 32/46, 02-668 Warszawa, Poland

‡ Institute of Experimental Physics, Warsaw University, ul Hoża 69, 00-681 Warszawa, Poland

Received 29 March 1989, in final form 9 June 1989

Abstract. Hyperfine structure in three $n^2D_{5/2}$ states ($n = 11$, 12 and 13) of ^{87}Rb was investigated by the quantum-beat method in zero magnetic field. The states of interest were excited by two-photon absorption from a single hyperfine substate (with $F = 1$) of the ground state. The magnetic-dipole interaction constant A and the electric-quadrupole interaction constant B were obtained by analysis of the modulation frequencies of the fluorescence signals (transition $n^2D_{5/2}$–$5^2P_{3/2}$). The results (MHz) are as follows: $|A(11^2D_{5/2})| = 0.361(7)$, $|B(11^2D_{5/2})| = 0.071(11)$, $|A(12^2D_{5/2})| = 0.266(9)$, $|B(12^2D_{5/2})| = 0.063(14)$, $|A(13^2D_{5/2})| = 0.20(1)$, $|B(13^2D_{5/2})| = 0.05(2)$. For all the states, A and B differ in sign. The effective lifetimes obtained as a by-product of the experiment are also presented.

1. Introduction

The first observations of quantum beats were reported by Aleksandrov (1964) and by Dodd *et al* (1964). The beats were associated with the Zeeman structure of the investigated levels. It was only after tunable lasers became available that the quantum-beat method was applied to the investigation of hyperfine structures (HFS). The first results on the subject were published by Haroche *et al* (1974), and concerned the HFS of the $7^2P_{3/2}$ state of caesium. Since then, the method has been used to determine the hyperfine stucture constants of several P and D states of alkali atoms. Measurements in potassium D states (Głódź and Kraińska-Miszczak 1985a, b) showed that analysis of quantum-beat signals makes the determination of the magnetic-dipole interaction constant A possible down to values comparable with the natural width of the levels and with an accuracy better than that obtainable using techniques such as optical double resonance or level crossing.

Our attempts to make use of the quantum-beat method to study the hyperfine structure of the $n^2D_{5/2}$ states of ^{87}Rb started with $n = 10$ (Głódź and Kraińska-Miszczak 1987). We obtained both the magnetic-dipole interaction constant A and the electric-quadrupole interaction constant B. Here, we report measurements dealing with higher n values: 11, 12 and 13. For lower states ($n = 4$–9), the values of A were determined by other authors and by different techniques: radiofrequency spectroscopy was employed for the $n^2D_{5/2}$ states with $n = 4$ by Lam *et al* (1980), with $n = 5$ by Tai *et al* (1975) and with $n = 8, 9$ by Belin *et al* (1976). In the case of $n = 6$ and $n = 7$, both

0953-4075/89/193109+09$02.50

level crossing and optical double resonance methods were applied (Svanberg and Tsekeris 1975, Hogervorst and Svanberg 1975). All the existing experimental data on the HFS of the $n^2D_{5/2}$ states of ^{87}Rb are summarised in table 2.

2. Excitation and detection

The nuclear spin of ^{87}Rb is equal to $\frac{3}{2}$, and so we have two hyperfine levels (with $F = 2, 1$) in the ground $5^2S_{1/2}$ state. These are split by approximately 6.8 GHz, which is comparable with the fine structure (FS) of the n^2D states investigated. The fine splitting for the 11^2D states of rubidium is known from measurements by Stoicheff and Weinberger (1979), and for the 12 and 13^2D states by Kato and Stoicheff (1976). Reported values of the fine-structure intervals (GHz) are 11.020 (30), 8.306 (34) and 6.456 (30), respectively.

In our experiment the excitation scheme had to account for relations between the FS of the excited state and HFS of the ground state. The $n^2D_{5/2}$ states were reached by two-photon absorption of laser light. The relative energies of the absorption components needed for excitation of the $n^2D_{3/2,5/2}$ states from the hyperfine split ground state are shown in figure 1. Using a spectral width of the pulsed dye laser employed in the experiment of about 3 GHz, we were able to excite selectively the $n^2D_{5/2}$ states in the transition starting from the $F = 1$ sublevel of the ground state—in figure 1 the d component, one that corresponds to the highest energy. Fluorescence to $5^2P_{3/2}$ was detected (see the inset in figure 3).

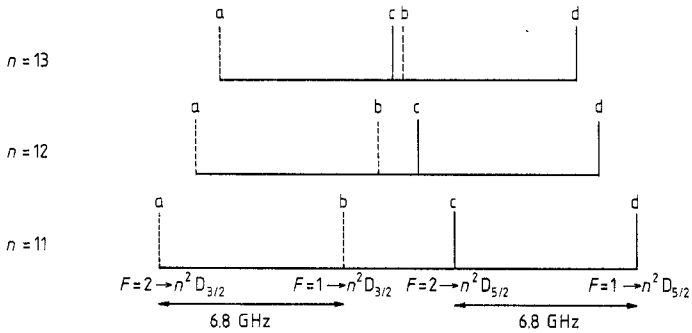

Figure 1. Fine-structure components in the $5^2S_{1/2}$-n^2D_J transitions including the hyperfine structure of the ground state.

The time-dependent signal $I(t)$ of the fluorescence from the hyperfine structure manifold coherently excited by a laser pulse exhibits modulation (quantum beats) with frequencies corresponding to the energy intervals between the hyperfine sublevels F' and F'':

$$I(t) = \left(X_0 + \sum_{\substack{F',F'' \\ F'>F''}} X_{F'F''} \cos(\omega_{F'F''} t) \right) \exp(-\Gamma t). \tag{1}$$

The amplitudes $X_{F'F''}$ of the modulation components depend on the geometrical and polarisation conditions of the experiment. The fluorescence signal is observed at right angles to both the direction of the laser light beam and to the direction of the electric field vector of this light. When the fluorescence component $I_{\parallel}$, linearly polarised

parallel to the polarisation of the exciting light, is detected (0° position of the polariser in the detection chain, called 'analyser'), the amplitudes $X_{F'F''}$ are twice those for the perpendicularly polarised $I_\perp$ component. These also differ in sign. Setting the transmission axis of the analyser at the 'magic angle' of 54.7°, an unmodulated signal is observed, decaying with lifetime $1/\Gamma$. We detected both modulated and unmodulated signals. For more details on the quantum-beat method, see e.g. the reviews by Haroche (1976) or by Dodd and Series (1978).

3. Experimental set-up

The experiment was performed in a sealed-off Pyrex cell containing isotopic rubidium (98% of ^{87}Rb and 2% of ^{85}Rb), kept at a temperature of 340 K. The corresponding atomic density was equal to 4.02×10^{17} m^{-3} (Gallagher and Lewis 1973). Special care was taken in preparation of the cell: it was subjected to several days of baking out at a temperature of 470 °C in a vacuum better than 10^{-7} Torr, before the metallic rubidium was distilled in.

A nitrogen laser-pumped dye laser was applied, giving light pulses of 4 ns duration. All three exciting laser wavelengths (615.1 nm, 611.2 nm and 608.2 nm, for $n=11$, 12 and 13, respectively) were in the lasing range of Rhodamine B. Tuning the laser, we observed, for each n, that the components of the excitation spectrum of the sequence, such as that in figure 1, were not well resolved. Therefore, during the experiment, we systematically controlled that excitation occurs at the 'blue wing' of the resonance corresponding to the d component, to ensure that the photons emitted originate only from the $n^2D_{5/2}$ state, excited from the $F=1$ substate of the ground state. Quantum beats were observed at fluorescence wavelengths 507.7 nm, 502.6 nm and 498.3 nm in $n^2D_{5/2}$-$5^2P_{3/2}$ transitions. For each wavelength, an interference filter with optimum transmission was selected.

The earth's magnetic field was cancelled to less than 20 mG by three pairs of orthogonal Helmholtz coils.

The fluorescence signal was registered as a function of time by the method of single-photon counting in delayed coincidence. As the time-to-amplitude converter can react to at most one photon following the laser pulse, a pile-up inspector discriminated against events in which more than one photon per pulse arrived. More details of the experimental method and of the apparatus are given in the papers on the HFS in the $10^2D_{5/2}$ level of ^{87}Rb (Głódź and Kraińska-Miszczak, 1985a, 1987).

4. Results and discussion

The excited $n^2D_{5/2}$ level consists of four hyperfine sublevels with $F=4$, 3, 2, 1. According to selection rules for two-photon absorption, $\Delta F\leqslant 2$, and due to the fact that excitation originated from one hyperfine sublevel (with $F=1$) of the ground state, three of these upper-state sublevels were accessible, namely those corresponding to $F=3$, 2 and 1. Modulation of the fluorescence signal was expected at three hyperfine frequencies. These frequencies in terms of the A and B constants are

$$\omega_{31}=5A-5B/4 \qquad \omega_{32}=3A-9B/20 \qquad \omega_{21}=2A-4B/5. \tag{2}$$

The contribution to the fluorescence originating from coherently excited pairs of $F'F''$ sublevels of the $n^2D_{5/2}$ state to common sublevels of the $5^2P_{3/2}$ state were calculated.

Only transitions with $\Delta m_F = 0$ were considered both in two-quantum absorption from the $5^2S_{1/2}$, $F=1$ ground state via the virtual $^2P_{3/2}$ state, and in fluorescence from the $n^2D_{5/2}$ to the $5^2P_{3/2}$ state. In this way, we obtained the relative amplitudes of the quantum beats and formula (1) can be expressed in a more explicit form:

$$I(t) = \{X_0 + X[\tfrac{1}{5}\cos(\omega_{31}t) + \tfrac{13}{9}\cos(\omega_{32}t) + \tfrac{7}{4}\cos(\omega_{21}t)]\}\exp(-\Gamma t). \qquad (3)$$

This formula, or its appropriate modification, was fitted to the experimental signals. The delay rate Γ either can be treated as one of the parameters to be fitted in formula (3), or can be determined from unmodulated decay curves (with the analyser at the 'magic angle'). An example of such an experimental decay curve, taken for $n = 13$, is shown in figure 2. The unmodulated curves were fitted to the formula $I(t) = X_0\exp(-\Gamma t) + \delta$, where δ stands for the noise background (noise was also accounted for in fitting the modulated signals to the experimental data, although no mention is later made of this detail).

The obtained Γ parameters will be referred to hereafter as Γ_{eff}. We consider these values to be effective ones for two main reasons. First, our values are not corrected for the influence of the black-body radiation, and secondly, even at this relatively low temperature (340 K) the effect of collisions may be non-negligible. The latter will be analysed later.

Values of $1/\Gamma_{\text{eff}}$ are given in table 1. The errors account for statistical error from the least-squares fitting procedure and for the influence of the uncertainty in the timescale. The values are compared with the theoretical lifetimes calculated by Theodosiou (1984) for rubidium temperatures close to that of our experiment. Results of Gounand *et al* (1980) are given as an example of experimental lifetimes. They were

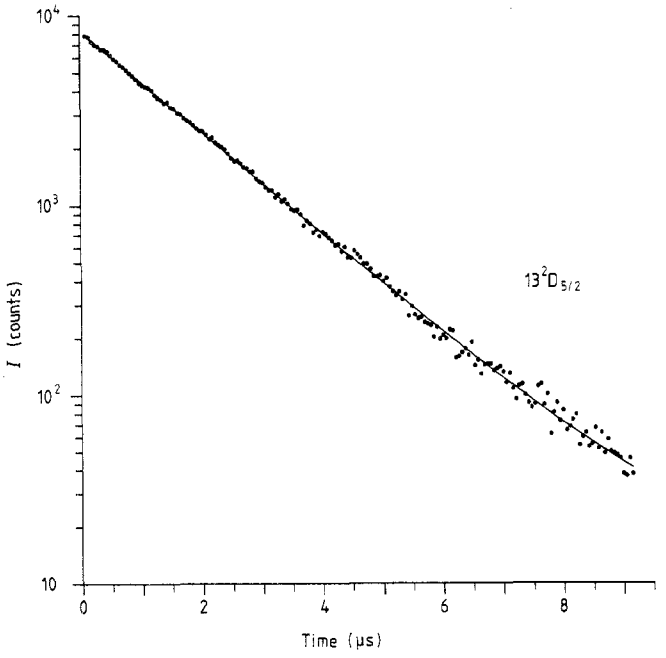

Figure 2. Unmodulated decay signal from the $13^2D_{5/2}$ state obtained with the analyser set at the magic angle (log-linear plot). The full curve is a least-squares fit to the points.

Table 1. Lifetimes ($1/\Gamma_{eff}$) of the $n^2D_{5/2}$ states of ^{87}Rb measured at a temperature of 340 K compared with experimental and theoretical values.

	Lifetime (ns)		
	Experiment		
State	This work, 340 K	Other[a], 520 K	Theory[b], 350 K
$11^2D_{5/2}$	1017 (25)	975 (200)	999.00
$12^2D_{5/2}$	1409 (40)	1250 (300)	1275.25
$13^2D_{5/2}$	1626 (40)	1400 (300)	1602.34

[a] Gounand *et al* (1980).
[b] Theodosiou (1984).

extrapolated to zero rubidium density and measured at the upper cell temperature of 540 K.

We should say that admixture of fluorescence from other transitions could be a possible source of systematic error in Γ_{eff}. The interference filters transmitted not only the lines of interest but also some fluorescence lines from the levels populated in cascades originating from the $n^2D_{5/2}$ states. Among them the $(n+1)^2S_{1/2}$–$5^2P_{1/2}$ and $(n-1)^2D_{3/2}$–$5^2P_{1/2}$ transitions are at wavelengths very close to those of the $n^2D_{5/2}$–$5^2P_{3/2}$ lines. An estimate made for $n=11$ on the basis of known transition probabilities (Lindgard and Nielsen 1977) showed, however, that these contributions are negligible. Assuming that this is also true for $n=12$ and 13 (we are not aware of data on relevant transition probabilities), a description of fluorescence in which these admixtures are neglected seems reasonable. Superradiant cascading (see Gounand *et al* 1979) might have changed the picture, but we have not seen any evidence of superradiance.

The main concern of further discussion will be to examine the problem of how a description of the decaying population could effect the values of HFS constants obtained by processing the modulated signals. Such modulated experimental signals of $I_{\parallel}$ from all the levels investigated are shown in figure 3. The other set ($I_{\perp}$) was also analysed.

As the starting point in the fitting procedure, formula (3) was fitted to the experimental points, and hence the A and B constants related by (2) to the three modulation frequencies were obtained. Formula (3) does not account for any collisional processes that may effect the shape of the decay. The cell was, as stated in § 2, carefully outgassed during its preparation to minimise the presence of impurities and measurements were performed at a rather low temperature. However, even at a density of rubidium atoms as low as that used in this experiment, the effect of collisional misalignment and depopulation may not be neglected. The effect would manifest itself in a two-exponential decay of population and in damping of the quantum beats with a damping parameter larger than the inverse of the natural lifetime (e.g. Pendrill and Series 1978). We unsuccessfully tried to fit the unmodulated fluorescence signals to the sum of two exponential functions. If two-exponential decay takes place, the two damping parameters do not differ enough to be distinguished. Thus, in the modified formula to be fitted to the $I_{\parallel}$ and $I_{\perp}$ signals, we assumed Γ_{eff} as an effective decay parameter for the population, but the damping rate of the beats was allowed to differ from Γ_{eff}, and was treated as a fitting parameter Γ_b. For all n the values of Γ_b obtained appeared to be slightly larger than Γ_{eff}, with a general tendency for Γ_b/Γ_{eff} to increase with increasing

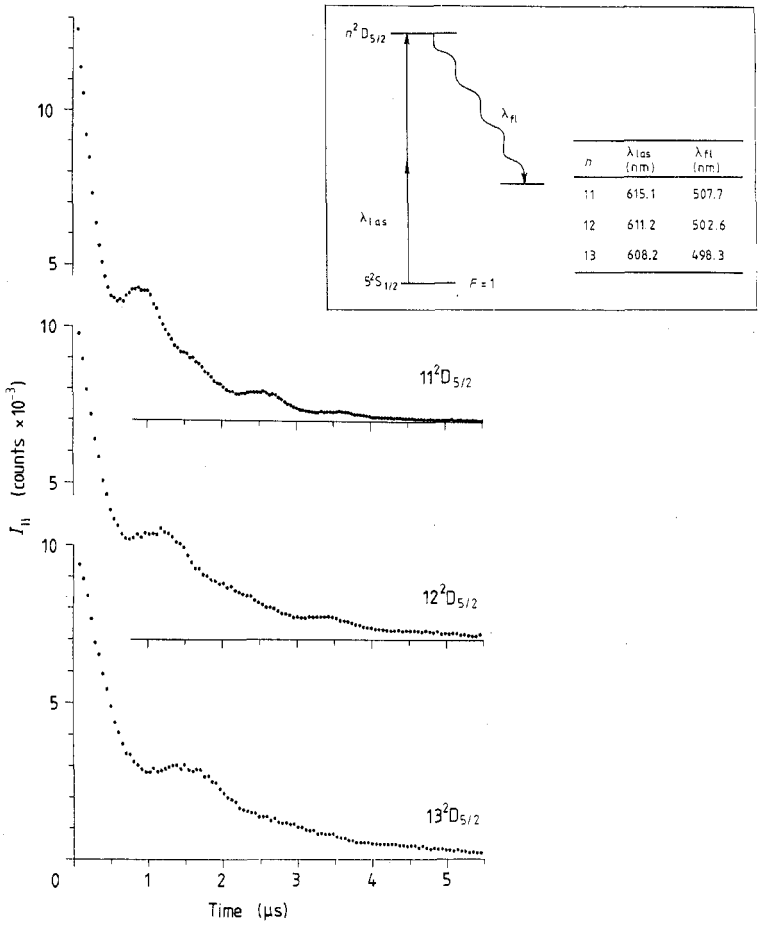

Figure 3. Quantum-beat signals from the $n^2D_{5/2}$ states of ^{87}Rb, fluorescence polarised parallel to the exciting laser light. The time range of data collection was equal to 7 μs for the $11^2D_{5/2}$ state, and 9 μs for the 12 and $13^2D_{5/2}$ states, although the plots are limited to 5.5 μs. The inset shows the excitation and detection scheme, and the wavelengths of the exciting laser light λ_{las} and the fluorescence λ_{fl}.

n. An example of a computer-fitted $I_{\parallel}$ curve, with $\Gamma_{eff} \neq \Gamma_b$, together with experimental points is shown in figure 4 ($11^2D_{5/2}$ state).

Allowance for additional damping of quantum beats led to smaller χ^2 values in the fitting procedure. For this reason, the values of A and B, presented in table 2 as the results of this experiment, are based on a formula modified in the above sense, rather than on (3). Nevertheless, the A and B values obtained previously (with (3)) are very close to the presented ones and fall well within the limits of estimated experimental errors given with the results in table 2.

These results are mean values of the ones obtained with two sets of data, $I_{\parallel}$ and $I_{\perp}$. Experimental data were fitted either to a formula in which ω_{ij} were expressed by A and B by relation (2) (so, A and B themselves were fitting parameters), or to a formula in which all three ω_{ij} were fitted—as if no relation between them existed and from the frequencies obtained the A and B values were recalculated. In the computational procedures, both formula (3) and that in which the beat amplitudes were treated

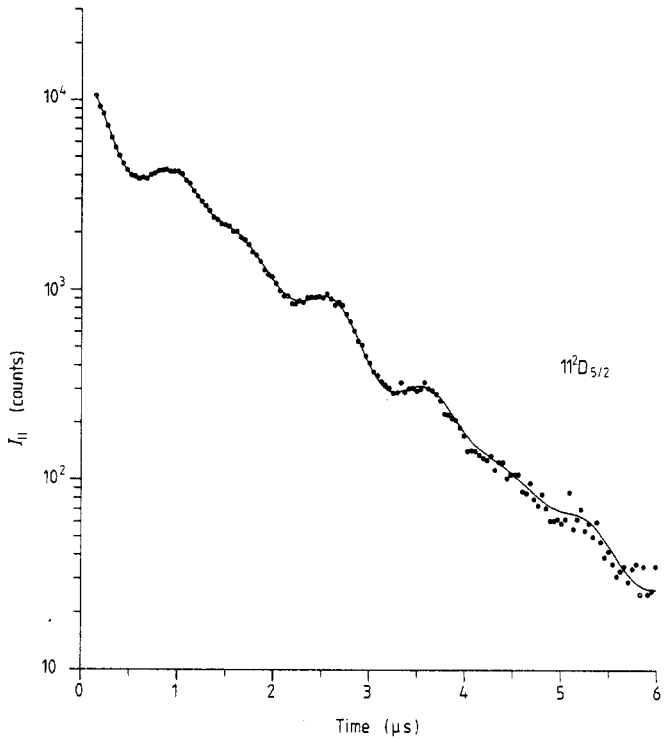

Figure 4. An example of a computer-fitted $I_{\parallel}$ curve, together with experimental points for the $11^2D_{5/2}$ state.

Table 2. Compilation of known experimental values of magnetic-dipole and electric-quadrupole interaction constants for the $n^2D_{5/2}$ states of ^{87}Rb.

State	A (MHz)	B (MHz)
$4^2D_{5/2}$	−16.9 (6)[a]	—
$5^2D_{5/2}$	−7.44 (10)[b]	—
$6^2D_{5/2}$	−3.4 (5)[c]	—
$7^2D_{5/2}$	−2.0 (3)[c]	—
$8^2D_{5/2}$	−1.20 (15)[d]	—
$9^2D_{5/2}$	∓0.80 (15)[d]	—
$10^2D_{5/2}$	∓0.510 (10)[e]	±0.096 (10)
$11^2D_{5/2}$	∓0.361 (7)[f]	±0.071 (11)
$12^2D_{5/2}$	∓0.266 (9)[f]	±0.063 (14)
$13^2D_{5/2}$	∓0.20 (1)[f]	±0.05 (2)

[a] Lam *et al* (1980).
[b] Tai *et al* (1975).
[c] Svanberg and Tsekeris (1975) and Hogervorst and Svanberg (1975).
[d] Belin *et al* (1976).
[e] Głódź and Kraińska-Miszczak (1987).
[f] Present work.

as fitting parameters were used. All these attempts gave very consistent results. The errors quoted account not only for the dispersion of the results—subject to averaging—but also for other uncertainties: in the origin of time, in the calibration of the timescale and in the decay parameter Γ_{eff}.

The quantum-beat method does not supply information on the signs of A and B constants; only their relative signs can be determined. We obtained $A/B<0$.

The resulting values of $|A|$ and $|B|$ are combined in table 2 with results of other experiments for the lower $^2D_{5/2}$ states in ^{87}Rb. All the known $|A|$ values are plotted in a log-log scale against the binding energy E_b of the respective $n^2D_{5/2}$ levels (figure 5). Full circles stand for results from this laboratory. The straight line drawn above the points represents the semiempirical rule stating a proportionality of $|A|$ with $E_b^{3/2}$ (Kopfermann 1958). It can be seen that in the $n^2D_{5/2}$ states of ^{87}Rb this rule is obeyed at least up to $n=13$.

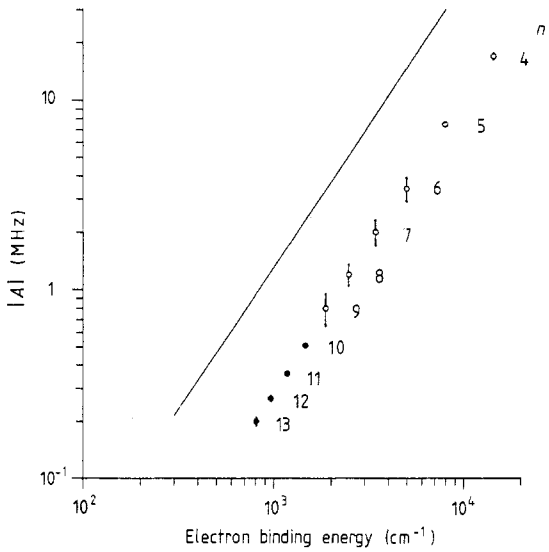

Figure 5. Experimental A constants for $n^2D_{5/2}$ states of ^{87}Rb ($n=4$–13) versus the binding energies.

Acknowledgment

This work was carried out under Research Project CPBP 01.06.

References

Aleksandrov E B 1964 *Opt. Spectrosc.* **17** 1957-60
Belin G, Holmgren L and Svanberg S 1976 *Phys. Scr.* **13** 351-62
Dodd J N, Kaul D M and Warrington D M 1964 *Proc. Phys. Soc.* **84** 176-8
Dodd J N and Series G W 1978 *Progress in Atomic Spectroscopy* part A, ed W Hanle and H Kleinpoppen (New York: Plenum) pp 639-77
Gallagher A and Lewis E L 1973 *J. Opt. Soc. Am.* **63** 864-9

Głódź M and Kraińska-Miszczak M 1985a *J. Phys. B: At. Mol. Phys.* **18** 1515-22
—— 1985b *Phys. Lett.* **110A** 203-5
—— 1987 *J. Phys. B: At. Mol. Phys.* **20** L541-5
Gounand F, Hugon M and Fournier P 1980 *J. Physique* **41** 119-21
Gounand F, Hugon M, Fournier P R and Berlande J 1979 *J. Phys. B: At. Mol. Phys.* **12** 547-53
Haroche S 1976 *High Resolution Laser Spectroscopy* ed K Shimoda (Berlin: Springer) pp 253-313
Haroche S, Paisner J A and Schawlow A L 1974 *Phys. Rev. Lett.* **32** 1333
Hogervorst W and Svanberg S 1975 *Phys. Scr.* **12** 67-74
Kato Y and Stoicheff B P 1976 *J. Opt. Soc. Am.* **66** 490-2
Kopfermann H 1960 *Nuclear Moments* (New York: Academic)
Lam L K, Gupta R and Happer W 1980 *Phys. Rev.* A **21** 1225-34
Lindgård A and Nielsen S E 1977 *At. Data Nucl. Data Tables* **19** 533-633
Pendrill L R and Series G W 1978 *J. Phys. B: At. Mol. Phys.* **11** 4049-57
Stoicheff B P and Weinberger E 1979 *Can. J. Phys.* **57** 2143-54
Svanberg S and Tsekeris P 1975 *Phys. Rev.* A **11** 1125-37
Tai C, Happer W and Gupta R 1965 *Phys. Rev.* A **12** 736-47
Theodosiou C E 1984 *Phys. Rev.* A **30** 2881-909